Role of Protein Phosphatase 2A in the Regulation of Endothelial Cell Cytoskeleton Structure

Krisztina Tar,[1,2] Csilla Csortos,[1,2] Istvan Czikora,[2] Gabor Olah,[1] Shwu-Fan Ma,[1] Raj Wadgaonkar,[1] Pal Gergely,[2] Joe G.N. Garcia,[1] and Alexander D. Verin[1]*

[1]Department of Medicine, Division of Biological Sciences, The University of Chicago, Chicago, Illinois
[2]Department of Medical Chemistry, Research Center for Molecular Medicine, University of Debrecen, Medical and Health Science Center, H-4026 Debrecen, Hungary

Abstract   Our recently published data suggested the involvement of protein phosphatase 2A (PP2A) in endothelial cell (EC) barrier regulation (Tar et al. [2004] J Cell Biochem 92:534–546). In order to further elucidate the role of PP2A in the regulation of EC cytoskeleton and permeability, PP2A catalytic (PP2Ac) and A regulatory (PP2Aa) subunits were cloned and human pulmonary arterial EC (HPAEC) were transfected with PP2A mammalian expression constructs or infected with PP2A recombinant adenoviruses. Immunostaining of PP2Ac or of PP2Aa + c overexpressing HPAEC indicated actin cytoskeleton rearrangement. PP2A overexpression hindered or at least dramatically reduced thrombin- or nocodazole-induced F-actin stress fiber formation and microtubule (MT) dissolution. Accordingly, it also attenuated thrombin- or nocodazole-induced decrease in transendothelial electrical resistance indicative of barrier protection. Inhibition of PP2A by okadaic acid abolished its effect on agonist-induced changes in EC cytoskeleton; this indicates a critical role of PP2A activity in EC cytoskeletal maintenance. The overexpression of PP2A significantly attenuated thrombin- or nocodazole-induced phosphorylation of HSP27 and tau, two cytoskeletal proteins, which potentially could be involved in agonist-induced cytoskeletal rearrangement and in the increase of permeability. PP2A-mediated dephosphorylation of HSP27 and tau correlated with PP2A-induced preservation of EC cytoskeleton and barrier maintenance. Collectively, our observations clearly demonstrate the crucial role of PP2A in EC barrier protection. J. Cell. Biochem. 98: 931–953, 2006.   © 2006 Wiley-Liss, Inc.

Key words: endothelium; phosphatase 2A; permeability; microtubules; microfilaments; tau; HSP27

Endothelial cells (EC) form a confluent monolayer on the surface of the inner wall of blood vessels and also participate in the regulation of many physiological and pathological processes. One of their major functions is the separation of blood from underlying tissues, allowing only tightly controlled passage of macromolecules and cells. Specialized transcellular systems of transport vesicles and the coordinated opening and closing of cell–cell junctions [Dejana, 2004] participate to maintain endothelial integrity, which is vital for the protection of vessels from uncontrolled increases in permeability or inflammation. Intercellular gap formation evoked by bioactive agents results in increased endothelial permeability, a typical feature of acute inflammatory lung syndrome [Garcia et al., 1986, 1995]. Gap formation and EC barrier integrity are governed by coordinated functioning of the components of the cytoskeleton. Reversible phosphorylation of numerous cytoskeletal proteins has a crucial role in the maintenance of appropriate alignment of the cytoskeleton [Dudek and Garcia, 2001]. Actomyosin interaction and cell contraction critically depend on the level of phosphorylation of myosin light chains (MLC) as it has been previously established [Garcia et al., 1986, 1995]. Increased MLC phosphorylation initiates F-actin stress fiber formation leading to

paracellular gap formation and finally resulting in EC barrier dysfunction. MLC phosphorylation level is determined by the balanced activities of MLC kinase [Verin et al., 1998; Birukov et al., 2001] and myosin phosphatase (MP) [Verin et al., 1995, 2001]. The latter enzyme belongs to the type 1 family of Ser/Thr protein phosphatases [Hartshorne et al., 1998; Kolosova et al., 2003].

Only a few studies have suggested the involvement of the other major type of Ser/Thr specific protein phosphatases, protein phosphatase 2A (PP2A) in maintaining EC cytoskeletal organization and barrier function [Diwan et al., 1997; Gabel et al., 1999; Knapp et al., 1999; Tar et al., 2004]. The PP2A holoenzyme consists of three subunits. The C catalytic (PP2Ac, 36 kDa), and A (PP2Aa, 65 kDa) structural subunits form the constant core of the enzyme. Both subunits have only two isoforms [Janssens and Goris, 2001]. However, the third subunit, commonly referred to as B subunit, has numerous protein families and each family has many isoforms [Csortos et al., 1996; Janssens and Goris, 2001]. Therefore, a large number of different holoenzyme forms may exist in the cells. Indeed, PP2A was described as participating in many cellular functions [Janssens and Goris, 2001].

Cytoskeletal targets of PP2A are not well characterized. Several possible substrates involved at the level of microfilaments or microtubules in barrier function are allowed, due to the high variability of the holoenzyme forms. PP2A is recognized as a protein phosphatase interacting with the microtubules (MT) and MT-associated proteins (MAPs), such as tau [Satillaro et al., 1981; Ishikawa et al., 1992; Moraga et al., 1993; Ferhat et al., 1996; Togel et al., 1998]. PP2A was also described as an enzyme, which dephosphorylates the small heat shock protein, HSP27. Small HSPs are proposed to regulate actin filament dynamics and to stabilize microfilaments, after their dissociation from large to small aggregates and phosphorylation in a p38 MAPK-dependent manner following exposure to stress [Lavoie et al., 1995; Guay et al., 1997; Huot et al., 1997; Clerk et al., 1998; Gusev et al., 2002].

Since the impact of both microfilaments and microtubules is thought to be equally important in maintaining cytoskeletal structure as well as EC barrier function [Lee and Gotlieb, 2003; Petrache et al., 2003], it seems valuable to clarify the substrates of PP2A both in microfila-

ments and microtubules; and to explore the regulatory pathways in the cytoskeleton mediated by PP2A.

We have recently published data suggesting that PP2A and its physiological substrates are involved in EC barrier regulation [Tar et al., 2004]. We have shown that PP2A has MT-like localization in human pulmonary artery EC (HPAEC). In addition, PP2A, tau and HSP27 are present in MT-enriched fractions, this indicates a functional complex formation between PP2A and the MT cytoskeleton. Inhibition of PP2A significantly potentiates the effect of MT inhibitor, nocodazole, on transendothelial electrical resistance (TER). It indeed suggests the involvement of activity of PP2A in MT-mediated EC barrier regulation. Nevertheless, the exact role of PP2A in EC barrier function is still to be explored.

We focused our present study on determining the role of PP2A in EC cytoskeleton, and to identify its cytoskeletal protein targets, which are involved in endothelial barrier function. We utilized mammalian expression vectors and adenoviral system to introduce PP2A subunits into EC to study the impact of the enzyme on the EC cytoskeleton structure, on barrier function, and on the phosphorylation level of substrate candidates, such as tau and HSP27.

MATERIALS AND METHODS

Reagents

Unless specified, reagents were obtained from Sigma (St. Louis, MO). Okadaic acid (sodium salt) was purchased from Calbiochem (San Diego, CA). Monoclonal antibodies against β-tubulin and HSP27 were purchased from CRP, Inc. (Covance Research Products Denver, PA). C-myc and HA-tag specific mono- and polyclonal antibodies were purchased from Santa Cruz Biotechnology, Inc. (Santa Cruz, CA); BD Living Colors peptide polyclonal antibody raised against GFP was from Clontech (Palo Alto, CA). Phospho-tau (pS262) polyclonal antibody was from Biosource International (Camarillo, CA). Phospho-HSP27 (pS82) specific polyclonal antibody was purchased from Cell Signaling Technology, Inc. (Beverly, MA). Texas Red-phalloidin and Alexa 350-, Alexa 488-, Alexa 594-conjugated secondary antibodies and antifade mounting medium were purchased from Molecular Probes (Eugene, OR). Mammalian expression vectors pCMV-HA (3.8 kb) and pcDNA3.1/

Myc-His (version A, 5.5 kb) were purchased from BD Biosciences, Clontech (Palo Alto, CA) and Invitrogen (Carlsbad, CA), respectively. AdEasy™ Adenoviral Vector System for adenovirus production was purchased from Stratagene (La Jolla, CA).

Cell Cultures

Human pulmonary artery endothelial cells (HPAEC), human umbilical vein EC (HUVEC), and human lung microvascular EC (HLMVEC) were obtained from Clonetics, BioWhittaker, Inc. (Frederick, MD) and were cultured in endothelial basal medium (EBM)-2 growth media supplemented with 0.2 ml of hydrocortisone, 2 ml of human FGF-B, 0.5 ml of VEGF, 0.5 ml of long-arm insulin-like growth factor-1 (R^3-IGF-1), 0.5 ml of ascorbic acid, 0.5 ml of human epidermal growth factor (EGF), 0.5 ml of GA-1000, and 0.5 ml of heparin (Clonetics)/500 ml with 10% FBS. All cells were maintained at 37°C in a humidified atmosphere of 5% CO_2 and 95% air [Petrache et al., 2003]. HPAEC were utilized at passages 6–10, HUVEC at passages 2–3, and HLMVEC at passages 4–8.

AD-293 cell line was obtained from Stratagene (La Jolla, CA). AD-293 cells were derived from the commonly used HEK293 cell line, but have improved cell adherence and plaque formation properties. HEK293 cells are human embryonic kidney cells transformed by sheared adenovirus type 5 DNA. AD-293 cells, like HEK293 cells produce the adenovirus *E1* gene allowing the production of infectious virus particles when cells are transfected with E1-deleted adenovirus vectors. Cells were cultured in DMEM (containing 4.5 g/L glucose and 110 mg/L sodium pyruvate and 2 mM L-glutamine), supplemented with 10% heat-inactivated fetal bovine serum. Cells were maintained at 37°C in a humidified atmosphere of 5% CO_2 and 95% air [Graham et al., 1977; He et al., 1998].

HUVEC cDNA Library Screening

HUVEC cDNA library screening was performed as it was previously described [Csortos et al., 1999]. Briefly, 10^6 clones of a random hexamer and oligo dT primed HUVEC λgt 11 cDNA library (kindly provided by Dr. David Ginsburg, Ann Arbor, USA) were screened. The RT-PCR amplified human liver PP2Ac, and the alfalfa PP2Aa subunit homolog (kindly provided by Dr. Viktor Dombrádi, University of Debrecen, Hungary) DNA probes were randomly primed, labeled with ^{32}P, and hybridization was carried out ($1–2 \times 10^6$ cpm/ml hybridization buffer) at 55°C with the immobilized clones. Labeled DNA probes bound non-specifically to the membrane were removed by washing with $2 \times$SSC at 60°C. Positive signals were detected by autoradiography. After at least three cycles of subsequent screening of the library the largest identified clones were tested by sequencing and the full length cDNAs for PP2Ac and PP2Aa were isolated/constructed using standard cloning methodologies.

Mammalian Expression Plasmids

The entire coding sequence of PP2Ac (930 bp) and PP2Aa (1770 bp) were amplified by PCR using the isolated HUVEC lambda phage clones as template. The 5′ end region of the specific oligonucleotide primer pairs contained appropriate restriction sites, *Sal* I (5′-TTGGTCG-ACCATGGACGAGAAGGTG-3′) and *Kpn* I (5′-GGGCGGTACCTTACAGGAAGTAGTCTG-3′) for PP2Ac; *Kpn* I (5′-AAGCATGGTACCATGG-CGGCGGCCGAC-3′) and *Xba* I (5′-GGGCTCT-AGAGGCGAGAGACAGAACAG-3′) for PP2Aa to subclone the PCR products into the mammalian pCMV-HA (PP2Ac) and pcDNA3.1/*Myc*-His (+) A version (PP2Aa) expression vectors. All constructs and their open reading frames were analyzed by sequencing using vector and PP2A specific primers.

In Vitro Phoshatase Activity Assay

^{32}P-labeled MLC were prepared by phosphorylation of 2 mg/ml MLC (MLC substrate was obtained courtesy of Dr. Ferenc Erdődi, University of Debrecen, Hungary) with 10 µg/ml MLCK in the presence of 15 µg/ml calmodulin, 0.2 mM $CaCl_2$, 0.25 mM [γ-^{32}P]ATP (600–1,000 counts/min/pmol) and 5 mM Mg-acetate at 30°C for 5 min. ^{32}P-MLC (~1 mol phosphate/mol MLC) was extensively dialyzed to remove the excess of ^{32}P-ATP [Kiss et al., 2002].

After transfection the cells were washed three times with $1 \times$ PBS, then lysed in lysis buffer (50 mM Tris, pH 7.5, 0.1 mM EDTA, 28 mM 2-ME, 0.5 mM PMSF, 2 mM benzamidine). To measure phosphatase activity, the samples were diluted 1:20 with buffer containing 20 mM Tris-HCl (pH 7.4), 0.1% 2-ME and 1 mg/ml BSA [Verin et al., 2000]. Since MLC is an in vitro substrate for both PP1 and PP2A, we used 5 nM okadaic acid, a specific inhibitor of PP2A at this

concentration [Cohen et al., 1990], to differentiate between PP1 and PP2A activities.

The amount of phosphatase was chosen in the assays as such that no more than 30% of the substrate would be converted during the incubation time (10 min at 30°C). The reaction was started by the addition of the substrate, and the released ^{32}P was determined according to the method of Erdodi et al. [1995]. Phosphatase activities were measured in the cell extracts of four independent transfections.

Transfection

Cells were grown to 70% of confluency, incubated with the appropriate PP2A subunit construct in the presence of FuGene 6 transfection reagent (Roche, Indianapolis, IN) according to manufacturer's protocol [Kolosova et al., 2004]. After 24 h of incubation the cells were washed 3× with 1× PBS and used for further experiments.

Adenoviral Plasmids

The entire coding sequences of PP2Ac and PP2Aa were subcloned into pShuttle-Ires-hrGFP-2-HA vector using *Eco* RV (5′-TGA-TATCCGATGTACCCATACGAT-3′) and *Sal* I (5′-GCGTCGACCTTACAGGAAGTAGTC-3′), or *Eco* RV (5′-ATTGATATCCGATGGCGGCG-GCC-3′) and *Xho* I (5′-GCTCTCGAGGGCGA-GAGACAG-3′) restriction sites, respectively. These restriction sites were created by PCR using appropriate primers. The entire coding sequences of the recombinants were verified by sequencing. Adenoviral recombinant plasmids were prepared with homologous recombination of the above plasmids with pAdEasy-1 viral DNA plasmid according to manufacturer's protocol (Stratagene, La Jolla, CA), and were verified by restriction analysis. As control, pShuttle-CMV-lacZ-pAdEasy-1 was used.

Viral Preparation

The virus was prepared according to the published methods [He et al., 1998] and manufacturer's protocol (Stratagene, La Jolla, CA) with slight modifications. Purified recombinant plasmids were linearized with the restriction enzyme *Pac* I, ethanol precipitated, and transfected into 50%−70% confluent AD-293 cells (2×10^6 cells/T-25 flask) using either LipoFectamine or FuGene and OptiMEM according to

the manufacturer's instructions. Transfection was confirmed by detection of GFP using a Nikon video-imaging system consisting of a phase contrast inverted microscope. Seven to 10 days post-transfection the cells were scraped off the plate in their culture medium. The harvested cells were collected, and resuspended in sterile PBS (2 ml/T-25 flask). The cells then were subjected to four rounds of freezing (dry ice/methanol), thawing (37°C), and vortexing (15 s at room temperature). The lysates were centrifuged at 500g for 5−10 min at 4°C. These crude viral preparations were then used to infect AD-293 cells (30%−50% of the viral supernatants/T-25 flask). Cells were harvested after 2−3 days in culture. Primary viral stocks produced were in the 10^7−10^8 pfu/ml range. After two rounds of infection using T-25 flasks, to further amplify the virus T-75 flasks were used. After another two rounds of infection high-titer viral preparation was performed. All cells were harvested, combined and spun for 5 min at 500g. The pellet was resuspended in 8 ml sterile PBS followed by four cycles of freeze/thaw/vortex processes. The lysate was centrifuged at 7,000g at 4°C for 5 min. Eight milliliters of the clarified supernatant were mixed with 4.4 g CsCl and centrifuged at 32,000 rpm, at 10°C for 7 h. The lower-band viral material was isolated, collected and dialyzed against three exchanges of TD buffer (137 mM NaCl, 6 mM KCl, 0.7 mM Na_2HPO_4, 25 mM Tris-HCl, pH 7.5) supplemented with 1 mM $CaCl_2$ and 1 mM $MgCl_2$. The purified virus (10^{10}−10^{11} pfu/ml) was aliquoted and stored with an equal volume of 2× storage buffer (10 mM Tris, pH 8.0, 100 mM NaCl, 0.1% BSA, and 50% glycerol, filter sterilized) at −20 or −70°C.

Transfected/infected cells containing the HA- and the GFP-tag were tested by Western blot analysis or immunostaining procedure.

Viral Infection

Serial dilutions of the purified virus were prepared in serum free medium. The media was aspirated from the plates of interest and replaced with the diluted virus. Complete medium containing serum and growth supplements were added 1 h later [see: Materials and Methods/Cell Culture; Yansong et al., 2000]. After overnight incubation the medium was changed again to complete medium and after 24 h of incubation, infected cells were used in further experiments.

Measurement of Transendothelial Electrical Resistance

The cellular barrier properties were monitored with a highly sensitive biophysical assay. The total electrical resistance was measured dynamically across the monolayer using an electrical cell-substrate impedance sensing system (Applied Biophysics, Troy, NY) described previously [Garcia et al., 1997; Schaphorst et al., 1997]. Decreases in monolayer resistance to electrical current flow, which correlated with paracellular gap formation were measured according to the method described by Giaever and Keese, 1993.

Western Immunoblotting

Cells for Western immunoblotting after transfection or infection protocols were washed three times with $1\times$ PBS then scraped from the dishes and lysed with two times boiling SDS sample buffer (125 mM Tris pH 6.8, 4% SDS, 10% glycerol, 0,006% bromophenol blue, 2% 2-mercaptoethanol), then passed through a 26-gauge needle. After 5 min boiling, the protein samples were centrifuged for 2 min and separated by SDS–PAGE [Laemmli, 1970] on 10% gels. Next the proteins were transferred to nitrocellulose membranes (30 V for 18 h or 90 V for 2 h) as described [Towbin et al., 1992], and incubated with specific antibodies of interest. Immunoreactive proteins were detected with enhanced chemiluminescent detection system (ECL) according to the manufacturer's directions (Amersham, Little Chalfont, UK).

Immunofluorescent Staining

After specific treatments, EC grown on glass coverslips were fixed in 3.7% formaldehyde solution in PBS for 10 min at 4°C, washed three times with PBS, permeabilized with 0.2% Triton X-100 in PBST for 30 min at room temperature, and blocked with 2% BSA in PBST for 30 min [Kolosova et al., 2004]. PBS/PBST was replaced by TBS/TBST when phospho-specific primary antibodies were employed. Incubation with antibodies was performed in the blocking solution for 1 h at room temperature. Alexa 350-, 488-, Alexa 594-conjugated secondary antibodies were used for immunodetection. Actin filaments were stained with Texas Red-phalloidin. After immunostaining procedures slides were analyzed using a Nikon video-imaging system consisting of a phase contrast inverted microscope connected to a digital camera and image processor. The images were recorded and processed using Adobe Photoshop program.

Confocal Laser Scanning Microscopy (CLSM)

Cell cultures prepared for immunofluorescent staining were imaged on a Zeiss LSM 410 confocal scanning laser microscope equipped with Helium/Neon (543) and Krypton/Argon (488, 647) laser detectors using 163–165 nm pinholes. Individual random fields were collected using a Plan-Apochromat $63\times/1.4$ oil DIC immersion objective lens [Lontay et al., 2004].

A Leica SP2 A OBS laser scanning confocal microscope (scanner with 2000-Hz line scans, frame scan rate of 40 fps at 512×32 pixels, scan resolution up to $4{,}096 \times 4{,}096$ pixels, zoom to $32\times$, scan rotation; interactive control panel with digital potentiometers) was also used for imaging protein co-localization. The scan detector was equipped with an acousto-optical beam splitter (AOBS) to select/introduce most excitation laser lines eliminating the need for main dichroic mirrors.

Total RNA Isolation

Total RNA from cultured endothelial cells was isolated using silica gel-based membrane with the RNeasy kit (Qiagen, Valencia, CA), according to the manufacturer's protocol (http://www1.qiagen.com).

Real-Time Reverse Transcriptase Polymerase Chain Reaction (Real-Time RT- PCR)

Transcription levels of the MT-associated protein tau were measured in 96-well microtiter plates with an ABI Prism 7700 Sequence Detector System (Perkin-Elmer/Applied Biosystems, Foster City, CA). TaqMan Gene Expression Assays (Cat. no. Hs00213491_m1) which recognizes the common exon–exon junctions of tau isoforms 1, 2, 3, and 4 were purchased from Applied Biosystems. TaqMan® rRNA Control Reagent was used as an endogenous control for normalization. Briefly, 50 ng total RNA and one-step TaqMan Gold RT-PCR Kit (Perkin-Elmer/Applied Biosystems, P/N N808-0232) were mixed together as recommended by the manufacturer's protocol (www.appliedbiosystems.com). Reverse transcription was performed at 48°C for 30 min followed by AmpliTaq Gold activation at 95°C for 10 min and by 40 PCR cycles of 94°C for 15 s and 60°C

for 1 min. Threshold cycle, C_t, which correlates inversely with the target mRNA levels was set as the cycle at which each fluorescent signal was first detected above background. Reactions without the reverse transcriptase or template were used to confirm the purity and specificity of all products. A relative standard curve method was used to calculate the tau mRNA level in each cell type (n = 3) and results expressed as relative abundance to 18S rRNA.

RESULTS

Effect of PP2Ac Overexpression on Actin Cytoskeleton in EC

We addressed the question to determine the exact role of PP2A in pulmonary arterial endothelial cell cytoskeleton arrangement. First we cloned the PP2Aa (scaffolding) and PP2Ac (catalytic) subunit from HUVEC cDNA library (see Materials and Methods). Sequence analyses of the clones revealed three differences of nucleotides in the PP2Aa clone compared to published mammalian/human nucleotide sequence (GenBank accession no. BC001537), one amino acid differed (D to V) in the protein sequence at position 315 compared to the published human protein sequence (GenBank accession no. AAH01537); two nucleotides difference was found in the PP2Ac clone compared

to the human nucleotide sequence (GenBank accession no. NM_002715); however at the level of amino acid sequence we did not find any changes compared to the published human sequence (GenBank accession no. NP_002706). Coding sequences of the two subunits were subcloned into mammalian expression vectors and transiently transfected into human pulmonary EC as described in "Materials and Methods." Western immunoblotting shows (Fig. 1) that the optimal transfection ratio for the PP2Aa subunit construct was 3:2 (µl transfection reagent: µg DNA) after 24 h post-transfection incubation time (Fig. 1A), while for PP2Ac 6:1 ratio is the best (Fig. 1B). In our experiments we used 24 h incubation time for both PP2Aa and PP2Ac; and 3:2 or 6:1 ratio, respectively.

Gap formation in EC results in barrier dysfunction and hyperpermeability. Actin structures are of critical importance in cell contraction and gap formation as stress fiber formation may lead to imbalance between tethering and contractile forces regulating cell shape. Our recent data linked PP2A activity with microtubule and F-actin cytoskeleton remodeling [Tar et al., 2004]. Therefore, we investigated the effect of the overexpressed PP2A subunits on F-actin cytoskeleton structure using non-transfected cells as inside controls in
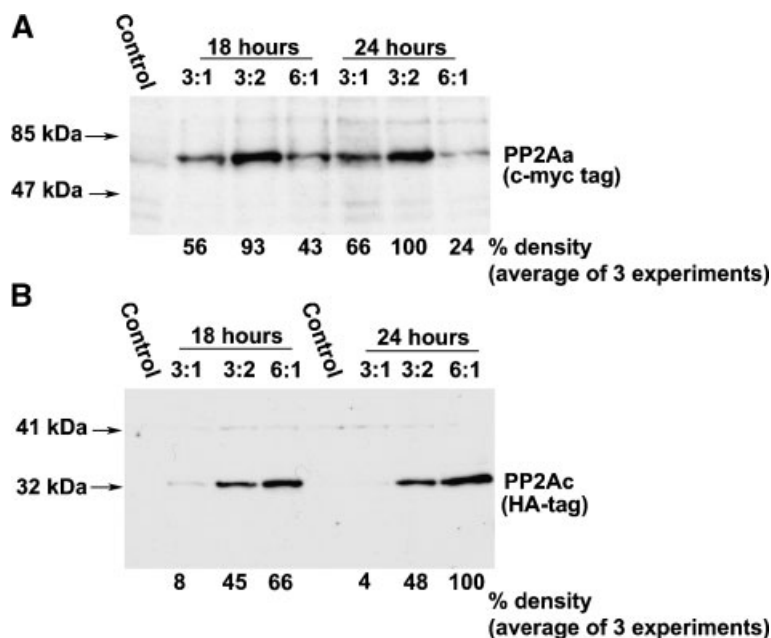
Fig. 1.   Overexpression of PP2A subunits in HPAEC. Western immunoblot detection of PP2Aa subunit (**A**), and PP2Ac subunit (**B**) overexpression in EC after different post-transfection time and FuGene (µl): DNA (µg) ratio. Transfection was performed as described in "Materials and Methods."

immunofluorescent imaging. Figure 2A–C show that overexpression of PP2Ac leads to actin cytoskeleton rearrangement; actin stress fibers, which span the cells, become dramatically thinner or almost completely disappear in the transfected cells. In contrast, the cortical actin ring on the cell periphery becomes thicker, suggesting that PP2Ac may be involved in stress fiber depolymerization as well as in cortical F-actin assembly. On the other hand, PP2Aa overexpression alone does not have a detectable effect on F-actin cytoskeleton in transfected cells (Fig. 2D–F). However, as Figure 2C and F, and their magnified insets demonstrate both subunits appear to co-localize with the peripherial F-actin region.

We also obtained slide images of the transfected EC by confocal microscopy. Distribution of overexpressed PP2Ac is observed in the nucleus and from the nucleus through the cytosol to the membrane; co-localization of F-actin and PP2Ac can mostly be detected in cell periphery (Fig. 2G). Confocal microscopy images also demonstrated the absence of actin fibers in the cytosol in PP2Ac overexpressing cells as we compare it to the neighboring control cells.

We detected similar disappearance of stress fibers and the enhancement of cortical actin ring when PP2Ac and PP2Aa were co-expressed (Fig. 3A–C).

In the next set of experiments we intended to clarify whether the overexpressed PP2A has any catalytic activity, and whether this activity could cause the above effect on F-actin cytoskeleton in ECs. Therefore, we measured the catalytic activity of overexpressed PP2A in in vitro phosphatase assay using ^{32}P-MLC as a substrate (see Materials and Methods). Since MLC is an in vitro substrate for both PP1 and PP2A, to differentiate between type 1 (PP1) and type 2A (PP2A) activities, assays were performed in the presence (only PP1 is active, PP2A is inhibited) or absence (both phosphatases are active) of 5 nM okadaic acid (OA), a Ser/Thr protein phosphatase inhibitor, specific for PP2A in this concentration [Cohen et al., 1990]. An approximately 30%–50% increase in PP2A activity was detected in PP2Ac transfected cell extracts compared to the controls (Table I).

Next we examined the effects of the inhibition of PP2A in cytoskeletal changes produced by PP2A overexpression in intact HPAEC. When

the cells were treated with OA [Wera and Hemmings, 1995], the F-actin cytoskeleton structure of ECs co-expressing PP2Ac and PP2Aa did not exhibit significant difference as compared to the surrounding non-transfected cells (Fig. 3D–F). This indicated that PP2A activity is crucial for PP2A-mediated actin remodeling.

Effect of the Overexpression of PP2Ac Subunit on Thrombin- or on Nocodazole-Induced EC Cytoskeletal Rearrangement

We studied the effect of thrombin and nocodazole to further elucidate the role of PP2A in EC cytoskeletal arrangement and barrier regulation on EC transfected with PP2A subunits. Thrombin is a recognized edemagenic agent [Garcia et al., 1986, 1995], and nocodazole is an MT inhibitor, both evoke stress fiber formation and barrier compromise [Verin et al., 2001]. Immunostaining of HPAEC for F-actin and either for PP2Ac (HA-tag) (Fig. 4A,B) or for PP2Aa (c-myc-tag) (Fig. 4C,D) demonstrates that PP2Ac transfection of ECs attenuated stress fiber formation induced by thrombin (50 nM for 30 min), but PP2Aa transfection did not have this kind of effect. Similarly, immunostaining of double-transfected HPAEC, with PP2Ac (HA-tag) and with PP2Aa (c-myc-tag) for F-actin demonstrates that PP2A overexpression significantly attenuated nocodazole-induced (200 nM, 30 min) stress fiber formation in EC compared to the surrounding non-transfected cells (Fig. 5A–C). More importantly, the inhibition of the activity of PP2A by okadaic acid (5 nM, 1.5 h) pre-treatment decreased this attenuating effect of PP2A transfection (Fig. 5D–F).

Our recent work [Tar et al., 2004] revealed tight connection between MT and PP2A, therefore we stained β-tubulin in PP2A transfected EC (Fig. 6) to visualize microtubules. Following nocodazole treatment (200 nM for 30 min) the structure of the microtubules was disrupted in non-transfected control cells, but remained uneffected in HPAEC overexpressing PP2Ac alone (Fig. 6A,B) or co-expressing PP2Ac and PP2Aa (Fig. 6E,F) demonstrating the stabilizing effect of PP2A on the MT structure. Cells co-expressing both A and C subunits were identified by the A-fusion c-myc-tag staining and the preserved MT staining of the cells. Inhibition of the activity of PP2A by the pre-treatment with

okadaic acid (5 nM for 1.5 h) completely abolished the effect of PP2A overexpression on nocodazole-induced MT dissolution indicating that the activity of PP2A is relevant to stabilize the MT (Fig. 6G–J).

Effect of Adenoviral Infection of PP2A on Agonist-Induced EC Permeability

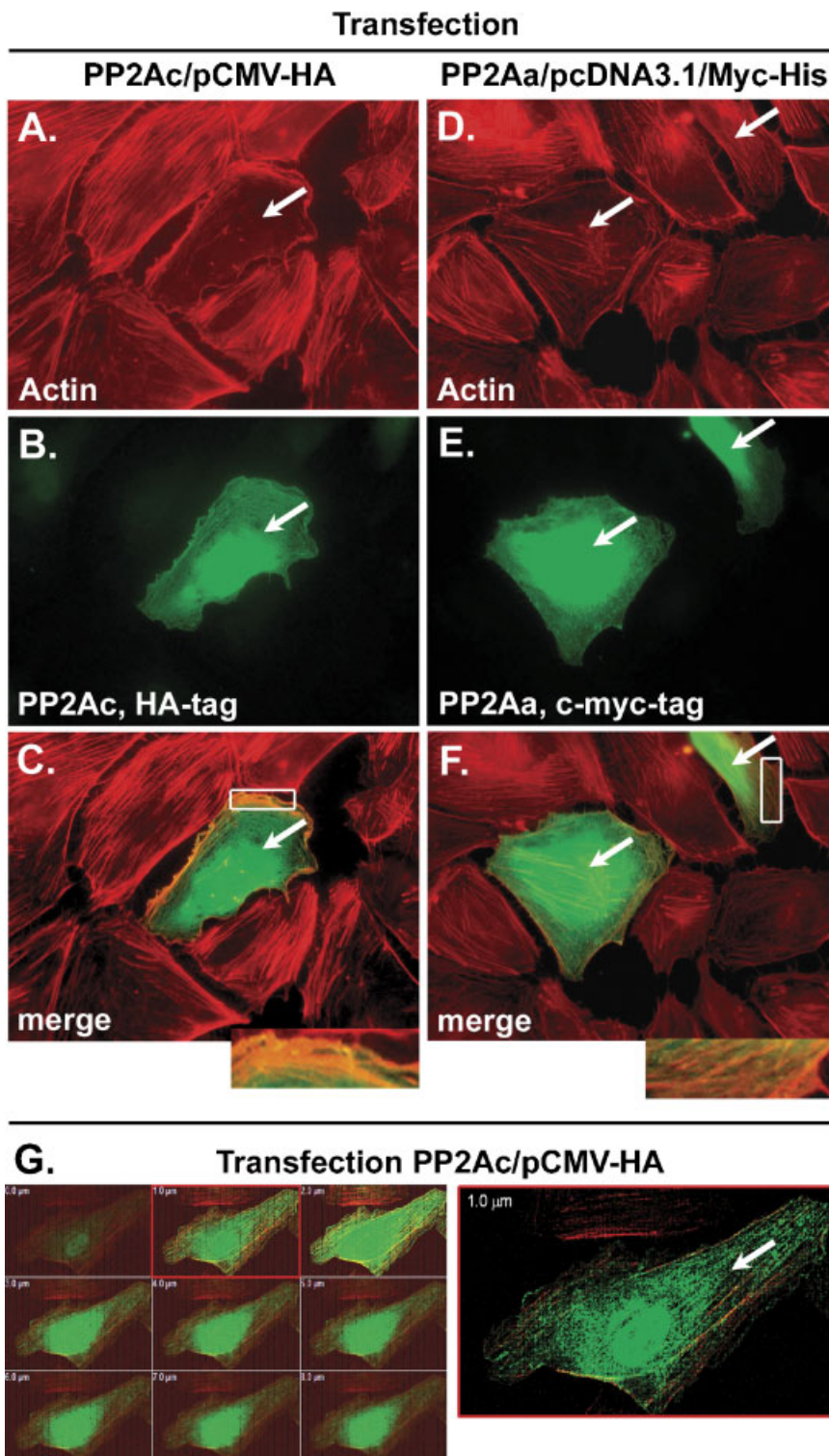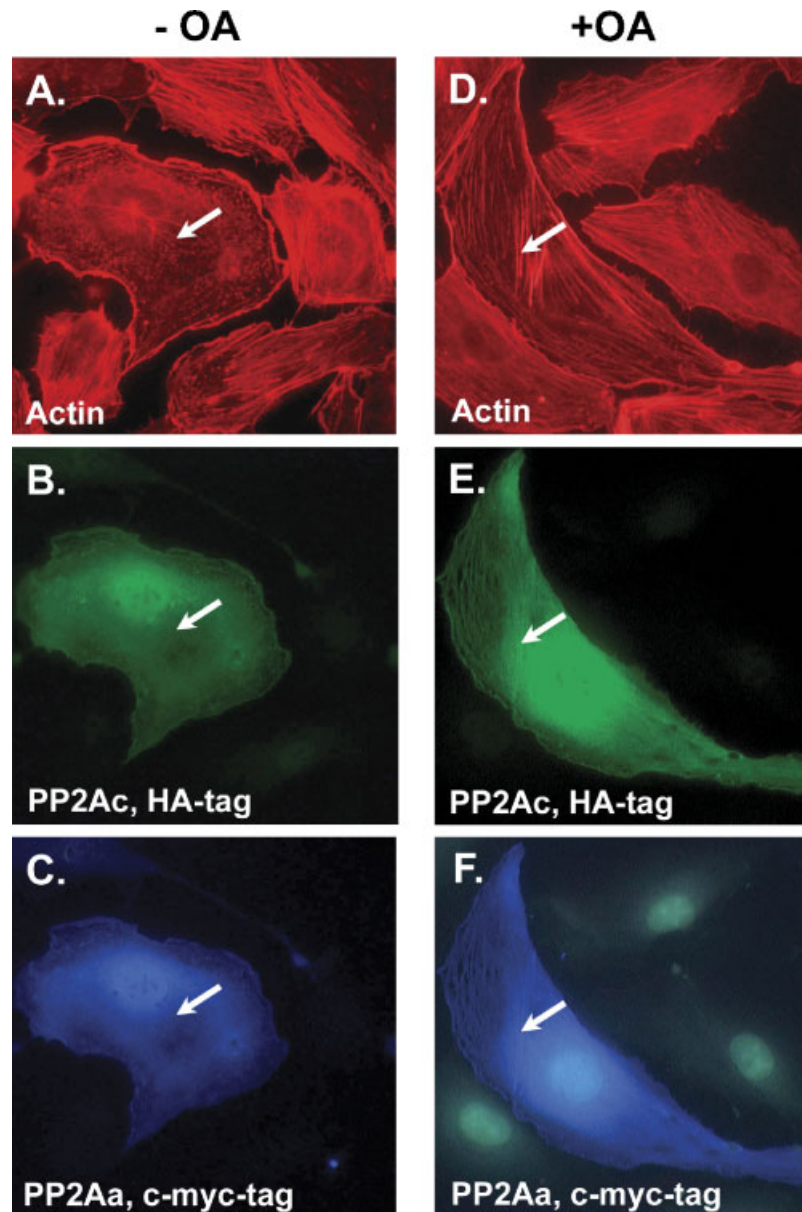The barrier function of EC can be monitored by a biophysical method; it detects the

Fig. 2.

Fig. 3. Inhibition of PP2A prevents actin redistribution. HPAEC were co-transfected with PP2Ac/pCMV-HA and PP2Aa/pcDNA3.1/c-Myc-His mammalian expression plasmids. The cells were treated with either vehicle (**A–C**), or 5 nM okadaic acid (**D–F**) for 1.5 h, and triple-stained to simultaneously visualize F-actin (red, A and D), PP2Ac (green, B and E), and PP2Aa (blue, C and F). Actin microfilaments were stained with Texas Red-phalloidin. Anti-HA tag polyclonal antibody and anti-c-myc monoclonal antibody were used to detect PP2Ac and PP2Aa, respectively. Cells expressing PP2Ac and PP2Aa are shown by arrows. A–C and D–F series are both parallel images of the same set of triple-stained cells. Shown are representative data of at least three independent experiments. [Color figure can be viewed in the online issue, which is available at www.interscience.wiley.com.]

Fig. 2. PP2Ac overexpression evokes actin cytoskeleton redistribution in endothelial cells. HPAEC were transfected with PP2Ac/pCMV-HA (**A–C**, **G**) or with PP2Aa/pcDNA3.1/Myc-His (**D–F**) mammalian expression plasmids. The cells were double-stained to visualize PP2Ac (green, B) or PP2Aa (green, E) simultaneously with F-actin (red, A and D). Actin microfilaments were stained with Texas Red-phalloidin. Anti-HA tag polyclonal antibody and anti-c-myc monoclonal antibody were used to detect PP2Ac and PP2Aa, respectively. A–B and D–E are both parallel images of the same set of double-stained cells. C: merge of A and B to visualize localization of F-actin and PP2Ac simultaneously. F: merge of D and E to show localization of F-actin and PP2Aa simultaneously. Insets represent enlarged peripheral regions (marked by white boxes) of EC. G: confocal images of HPAEC overexpressing PP2Ac. The images represent z serial sections with an individual slice thickness of 0.7–1.2 μm. Cells expressing PP2Ac or PP2Aa are shown by arrows. Shown are representative data of at least 3 independent experiments. [Color figure can be viewed in the online issue, which is available at www.interscience.wiley.com.]

TABLE I. In Vitro PP2A Activity Measurement in HPAEC

	PP2A activity, %
Vector control	100 ± 11
PP2Ac	147 ± 14
PP2Aa	106 ± 10
PP2Aa + c	166 ± 17

Phosphatase activity was measured with ^{32}P-MLC substrate as described in Materials and Methods. Average phosphatase activity values determined in four independent experiments are expressed in the percentage of vector control $\pm$ SD.

transendothelial electrical resistance (TER) of the EC monolayers. Cell retraction evokes increased permeability. Rounding or loss of adhesion is reflected by a decrease in TER [Giaever and Keese, 1993]. The transfection level of endothelial cells with the mammalian expression constructs is too low (10%–20%) to examine TER [Tanner et al., 1997], therefore we generated adenoviral recombinant constructs for PP2Ac and PP2Aa as described in Materials and Methods. The presence of overexpressed proteins in the infected EC was confirmed by Western blot analysis of the cell lysates (Fig. 7A,B) using anti-HA-tag and anti-GFP antibodies. High infection efficiency (~100%) was demonstrated by immunofluorescent staining with anti-HA-tag antibody (Fig. 7C).

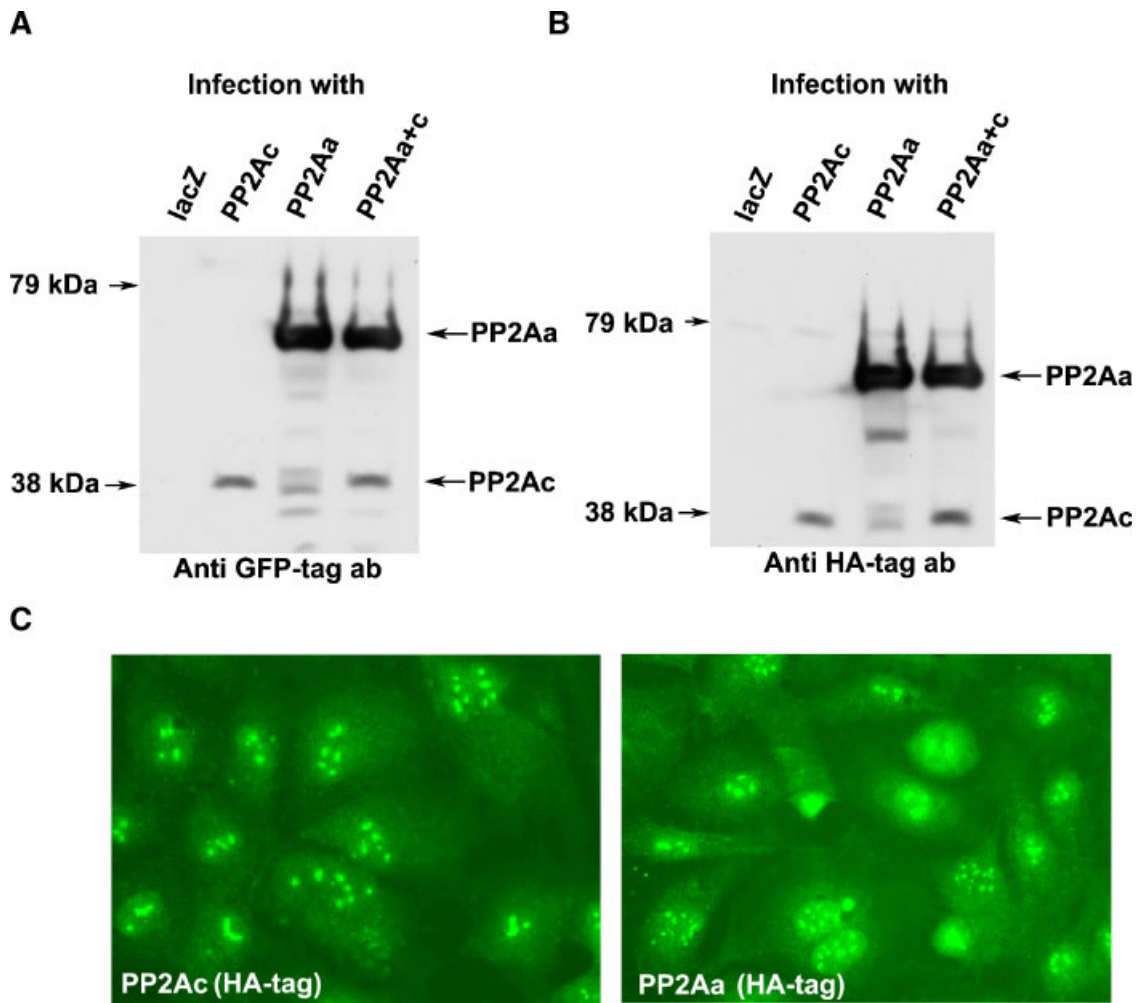We examined the effect of PP2A overexpression on thrombin-induced changes in TER.
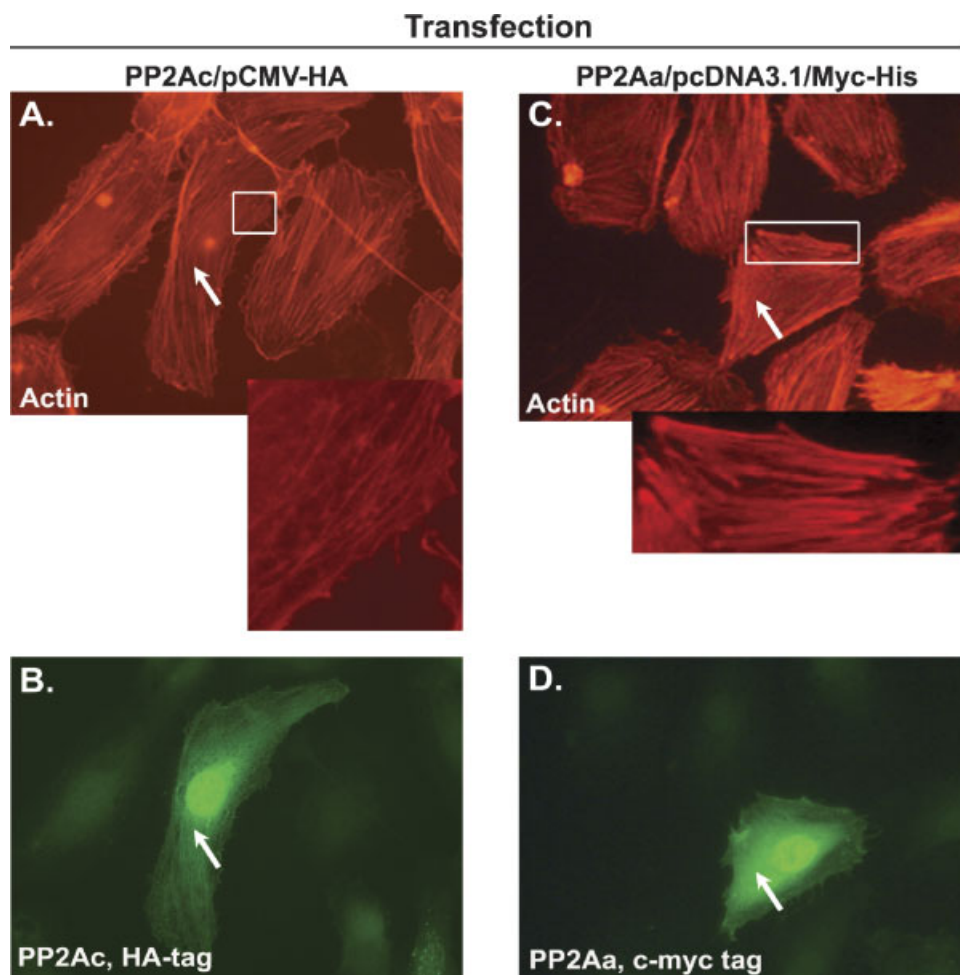
Fig. 4. PP2A overexpression attenuates the effect of thrombin. HPAEC were transfected with PP2Ac/pCMV-HA (**A–B**) or PP2Aa/pcDNA3.1/Myc-His (**C–D**) mammalian expression plasmid. The cells were treated with 50 nM thrombin for 30 min, and double-stained to simultaneously visualize F-actin (red, A and C), PP2Ac (green, B), or PP2Aa (green, D). Actin microfilaments were stained with Texas Red-phalloidin. Anti-HA tag polyclonal antibody and anti-c-myc monoclonal antibody were used to detect PP2Ac and PP2Aa, respectively. Cells expressing PP2Ac or PP2Aa are shown by arrows. A–B and C–D are both parallel images of the same set of double-stained cells. Insets represent enlarged regions (marked by white boxes). Shown are representative data of at least three independent experiments. [Color figure can be viewed in the online issue, which is available at www.interscience.wiley.com.]

Fig. 5. PP2A overexpression attenuates the effect of nocoda-zole on F-actin cytoskeleton. HPAEC were co-transfected with PP2Ac/pCMV-HA and PP2Aa/pcDNA3.1/Myc-His mammalian expression plasmids. The cells were treated with either vehicle (**A–C**), or 5 nM okadaic acid (**D–F**) for 1.5 h, after that with 200 nM nocodazole for 30 min (A–F), and triple-stained to simultaneously visualize F-actin (red, A and D), PP2Ac (green, B and E), and PP2Aa (blue, C and F). Actin microfilaments were stained with Texas Red-phalloidin. Anti-HA tag polyclonal antibody and anti-c-myc monoclonal antibody were used to detect PP2Ac and PP2Aa, respectively. Cells expressing PP2Ac and PP2Aa are shown by arrows. A–C and D–F series are both parallel images of the same set of triple-stained cells. Insets represent enlarged regions (marked by white boxes). Shown are representative data of at least three independent experiments. [Color figure can be viewed in the online issue, which is available at www.interscience.wiley.com.]

Fig. 6. PP2A overexpression stabilizes MT in HPAEC. HPAEC were transfected with PP2Ac/pCMV-HA (**A–B**), with PP2Aa/pcDNA3.1/Myc-His (**C–D**), or co-expressed with both (**E–J**) mammalian expression plasmids. A–F: cells were treated with 200 nM nocodazole for 30 min. G–J: cells were pretreated with 5 nM okadaic acid for 1.5 h, then treated with either vehicle (G, H), or 200 nM nocodazole (I, J). After the treatment the cells were double-stained to visualize PP2Ac (red, B, H, J) or PP2Aa (red, D, F) simultaneously with β-tubulin (green, A, C, E, G, I). Anti-HA-tag, and anti-c-myc-tag polyclonal, and anti-β-tubulin monoclonal antibodies were used to detect PP2Ac, PP2Aa, and β-tubulin, respectively. Cells expressing PP2Ac and/or PP2Aa are shown by arrows. A–B, C–D, E-F, G–H and I–J are all parallel images of the same set of double-stained cells. Shown are representative data of at least three independent experiments. [Color figure can be viewed in the online issue, which is available at www.interscience.wiley.com.]

Fig. 7. Adenoviral infection of HPAEC. HPAEC were grown to 90% confluency then infected with recombinant adenoviral constructs of PP2Ac, PP2Aa, or both. After 24 h incubation Western-blot analysis of the infected cells were performed; **A**: GFP-tag of recombinant proteins was detected by anti-GFP polyclonal antibody, and **B**: HA-tag of recombinant proteins was detected by anti-HA polyclonal antibody. **C**: Overexpression was also detected by immunofluorescent staining for PP2Ac and PP2Aa with anti-HA-tag polyclonal antibody. [Color figure can be viewed in the online issue, which is available at www.interscience.wiley.com.]

HPAEC infected with either lacZ control or PP2Ac + PP2Aa recombinant adenoviruses (see Materials and Methods) were treated with either vehicle (0.1% DMSO), or thrombin (20 nM) at 1 h of TER measurement, followed by monitoring TER for additional 5 h. Figure 8A demonstrates that thrombin increases permeability alone, but the infection of EC with adenoviral PP2A constructs significantly attenuated thrombin-induced decrease in TER. This indicates the direct involvement of PP2A in barrier protection against thrombin-induced EC barrier compromise. Similarly, PP2A overexpression attenuated the effect of nocodazole

(200 nM added at 30 min) on EC permeability (Fig. 8B).

Effect of the Overexpression of PP2A on Nocodazole/Thrombin-Induced Phosphorylation of Cytoskeletal Proteins

We have recently shown the association of the regulatory cytoskeletal protein, HSP27, with MT fractions in EC by Western blot [Tar et al., 2004]. Other studies also suggested that an increase in HSP27 phosphorylation level seems to lead to actin polymerization through the p38 MAP-kinase signaling pathway [Larsen et al.,

A

B
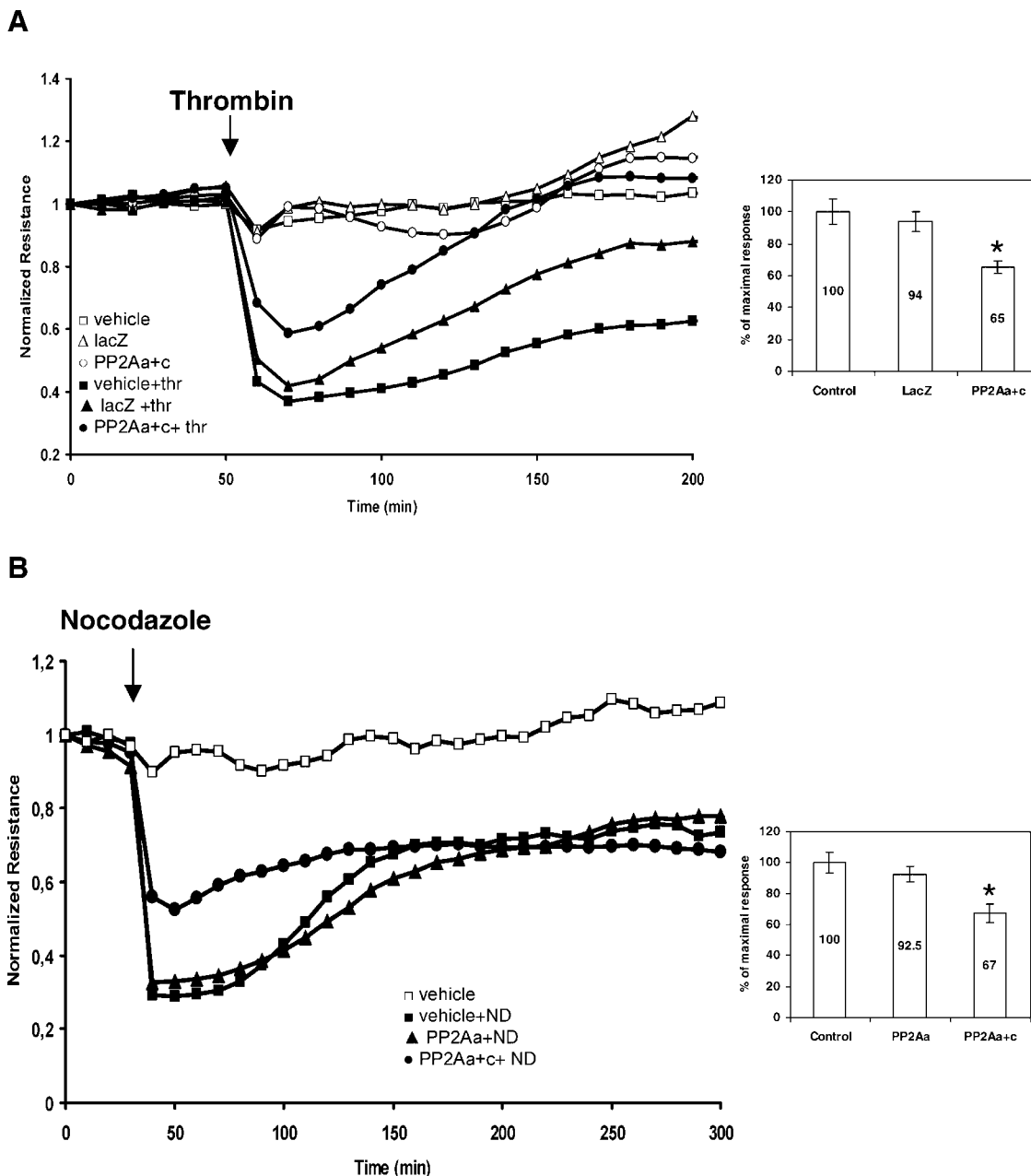
Fig. 8. The impact of thrombin and nocodazole on TER is smaller in PP2A-infected cells. HPAEC were infected with either PP2Aa-GFP, lacZ (both used as control), or PP2Ac-GFP; or double infected with PP2Aa-GFP and PP2Ac-GFP adenoviral constructs as described in Materials and Methods and were treated with either 0.1% DMSO (vehicle), 20 nM thrombin (**A**) or 200 nM nocodazole (**B**). TER was monitored for 5 h as described in Materials and Methods. Initial resistance values varied between 800 and 1,200 Ω. Normalized resistance values are shown. Solid arrows indicate the time of agonist addition. Results are from three representative experiments. A: □ vehicle treated with 0.1% DMSO, △ pShuttle-CMV-lacZ-pAdEasy-1 infected cells, ○ pShuttle-Ires-hrGFP-2-HA–PP2Aa + pShuttle-Ires-hrGFP-2-HA–PP2Ac double infected cells, ■ vehicle treated with 20 nM thrombin, ▲ pShuttle-CMV-lacZ-pAdEasy-1 infected cells treated with 20 nM thrombin, ● pShuttle-Ires-hrGFP-2-HA–PP2Aa + pShuttle-Ires-hrGFP-2-HA–PP2Ac double infected cells treated with 20 nM thrombin. B: □ vehicle treated with 0.1% DMSO, ■ vehicle treated with 200 nM nocodazole, ▲ pShuttle-Ires-hrGFP-2-HA–PP2Aa infected cells treated with 200 nM nocodazole, ● pShuttle-Ires-hrGFP-2-HA–PP2Aa + pShuttle-Ires-hrGFP-2-HA–PP2Ac double infected cells treated with 200 nM nocodazole. Insets show the percentage of maximal effect of thrombin (A) or nocodazole (B) on normalized resistance (average of three independent experiments).

1997; Schafer et al., 1998; Hedges et al., 1999]. HPAECs were co-transfected with PP2Ac and PP2Aa, and treated with nocodazole (200 nM, 30 min) or thrombin (20 nM, 30 min) to clarify the linkage between HSP27 dephosphorylation and the activity of PP2A. Immunostaining for phospho-HSP27, F-actin, and PP2Aa (c-myc-tag) indicated that PP2A-transfected cells following nocodazole or thrombin treatment contained significantly less phospho-HSP27 compared to non-transfected controls (Fig. 9). Overexpression of PP2Ac or co-expression of
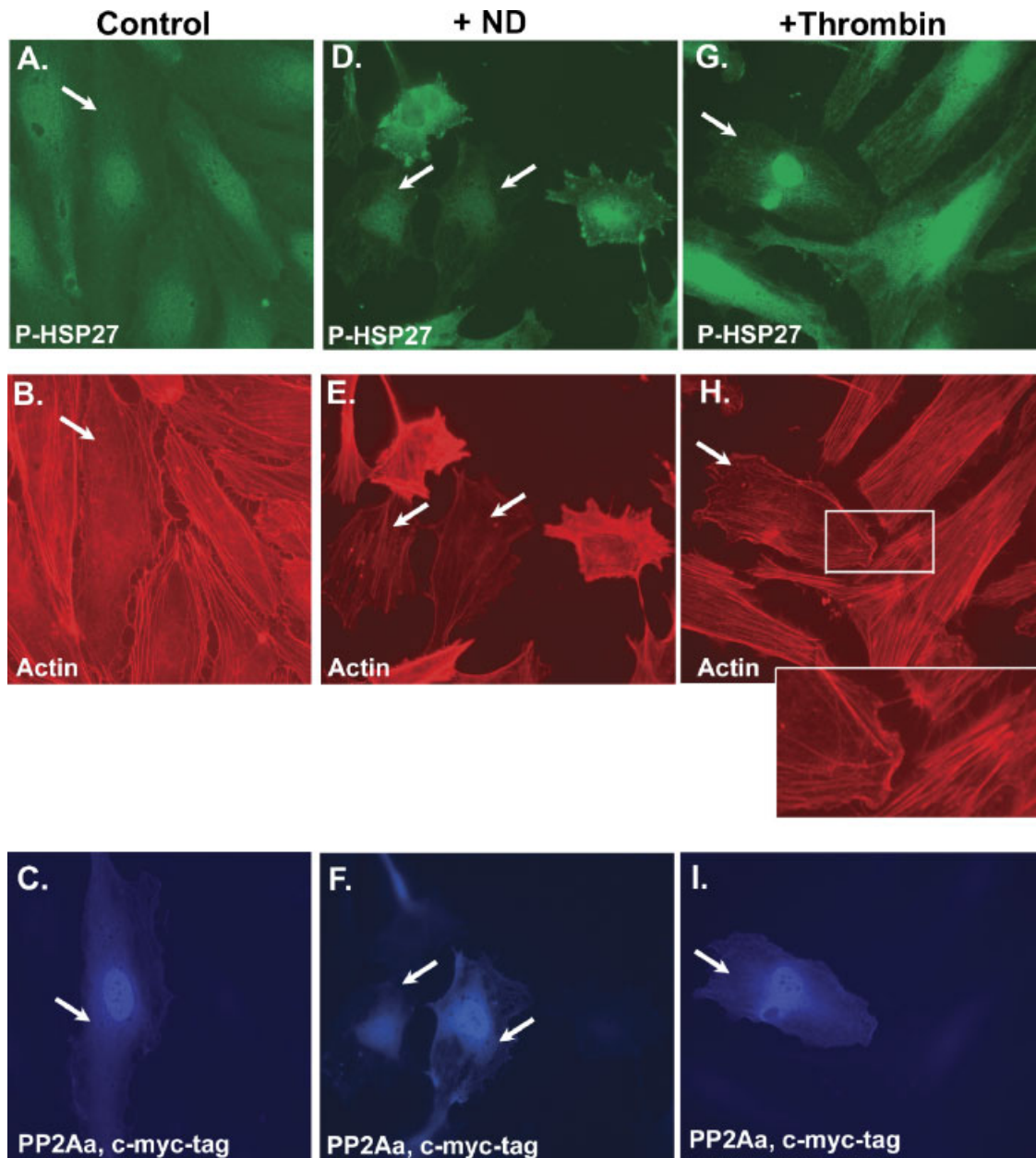
Fig. 9. PP2Ac overexpression attenuates HSP27 phosphorylation evoked by nocodazole or thrombin treatment. HPAEC were co-transfected with PP2Ac/pCMV-HA and PP2Aa/pcDNA3.1 mammalian expression plasmids. The cells were treated with either vehicle (**A–C**), or with 200 nM nocodazole for 30 min (**D–F**), or with 20 nM thrombin for 30 min (**G–I**), and triple-stained to simultaneously visualize P-HSP27 (green, A, D, and G), F-actin (red, B, E, and H), and PP2Aa (blue, C, F, and I). Actin microfilaments were stained with Texas Red-phalloidin. Anti-phospho-HSP27 (pS82) polyclonal and anti-c-myc monoclonal antibodies were used to detect P-HSP27 and PP2Aa, respectively. The A–C, D–F, and G–I series are parallel images of the same set of triple-stained cells. Cells expressing PP2Ac and PP2Aa are shown by arrows. Inset represents enlarged region (marked by white box). [Color figure can be viewed in the online issue, which is available at www.interscience.wiley.com.]

PP2Aa and PP2Ac changes the appearance of actin cytoskeleton; however the overexpression of the PP2Aa subunit alone does not change the actin structure (see Fig. 2A,D) in HPAEC. Therefore cells co-expressing both A and C subunits were identified 1) by the A subunit fusion c-myc-tag staining and 2) by the typical low-level F-actin staining of C subunit over-expressing cells. Both PP2A subunits co-expression does not change the level of HSP27 phosphorylation, but it leads to the disappearance of stress fibers in untreated HPAECs as it is demonstrated in Figure 9A–C. Nocodazole, or thrombin-induced increase of HSP27 phosphorylation level was observed in the non-transfected control cells, however there was no increase in the PP2A-overexpressing cells (Fig. 9D,G), and they maintained the original actin cytoskeleton arrangement even after the nocodazole/thrombin treatment (Fig. 9E,H).

In addition, our recently published data suggested [Tar et al., 2004] that PP2A could be involved in the determination of the phosphorylation level and the subcellular localization of the MT-associated protein tau, in EC. Inhibition of PP2A by okadaic acid treatment of EC increased the level of tau phosphorylation; and the majority of the phospho-tau protein was detected in the cytosol fraction with Western blot analysis [Tar et al., 2004]. However, the level of tau expression in EC was still to be determined. To evaluate the level of tau expression in various endothelial cell types, we used the real time RT-PCR method which allows the detection of PCR amplification during the early exponential growth phase therefore provides a distinct advantage over traditional PCR detection where the PCR amplification at the final phase or end-point is detected. Our results showed that HPAEC expresses the highest amount of tau mRNA level as compared to the other tested cell types (Fig. 10) suggesting that tau may participate in the arrangement of HPAEC cytoskeleton.

Immunostaining of untreated HPAEC with anti-phospho-tau antibody indicates equally low level of phospho-tau in both PP2A over-expressing and control cells (Fig. 11A–C). It is present in the cytosol and in the nucleus, however MT-like distribution cannot be observed. This is consistent with our recently published data [Birukova et al., 2004]. Nocodazole (200 nM, 30 min), or thrombin (20 nM, 30 min) treatment evoked an increase in the phosphor-
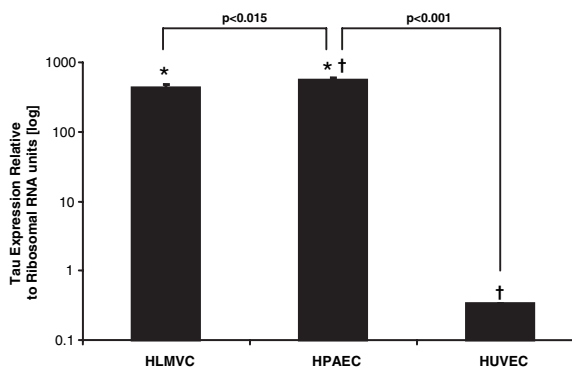
Fig. 10. Detection of tau expression levels in various human endothelial cells by real-time RT-PCR. Transcript abundance of tau in human lung microvascular EC (HLMVC); human pulmonary artery EC (HPAEC) and human umbilical vein EC (HUVEC) was determined by real time RT-PCR as described in Materials and Methods. Results were normalized to corresponding 18S rRNA intensity, relative abundance of tau was calculated and log transformed. Significance of differences in the abundance of tau between HPAEC and other cell types was evaluated by unpaired t-test. Error bars represent standard deviation derived from three individual experiments.

ylation level of tau in the control cells. However, the phosphorylation level of tau did not change in PP2A overexpressing cells (Figs. 11D–F and 12). Our confocal images shown in Figure 12 suggest co-localization of PP2A and phospho-tau in thrombin treated cells. This suggests that PP2A is able to dephosphorylate tau in HPAEC.

DISCUSSION

The results of our recent study suggested that PP2A, and its physiological substrates are involved in EC barrier regulation and that PP2A may participate in the regulation of endothelial cell permeability [Tar et al., 2004]. In this report we provide additional new data regarding the possible function of PP2A in EC.

To further clarify the role of PP2A in the regulation of EC cytoskeleton structure we cloned and prepared mammalian expression plasmids of the catalytic C subunit (PP2Ac) and the regulatory A subunit (PP2Aa). HPAEC were transfected with the recombinant expression plasmids. Previous reports indicated problematic overexpression of PP2Ac, since it is a tightly regulated protein [Baharians and Schonthal, 1998]. However, functional expression of PP2Ac was achieved with an N-terminal HA-tag [Wadzinski et al., 1992]. Therefore we
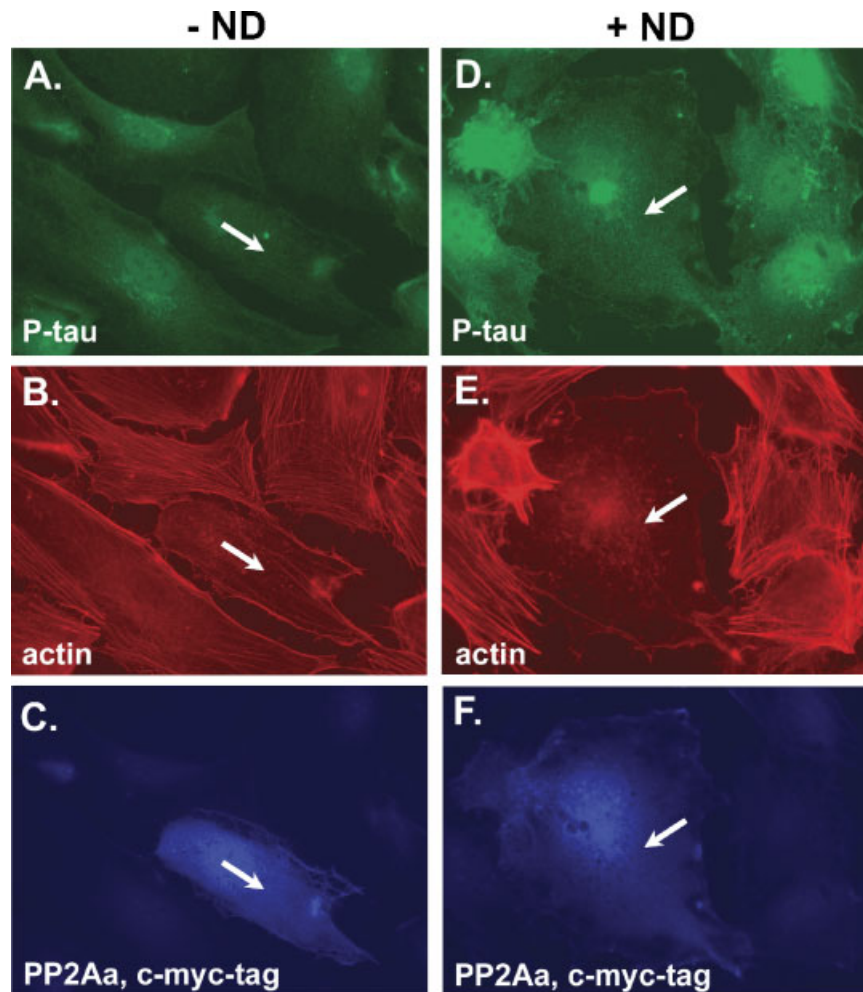
Fig. 11. PP2Ac overexpression attenuates tau phosphorylation evoked by nocodazole treatment. HPAEC were co-transfected with PP2Ac/pCMV-HA and PP2Aa/pcDNA3.1 mammalian expression plasmids. The cells were treated with either vehicle (**A**–**C**), or with 200 nM nocodazole for 30 min (**D**–**F**), and triple-stained to simultaneously visualize P-tau (green, A and D), F-actin (red, B and E), and PP2Aa (blue, C and F). Actin microfilaments were stained with Texas Red-phalloidin. Anti- phospho-tau (pS262) polyclonal and anti-c-myc-tag monoclonal antibodies were used to detect P-tau and PP2Aa, respectively. The A–C and D–F series are parallel images of the same set of triple-stained cells. Cells expressing PP2Ac and PP2Aa are shown by arrows. Shown are representative data of at least three independent experiments. [Color figure can be viewed in the online issue, which is available at www.interscience.wiley. com.]

performed transient expressions with 24 h post-transfection time; and for the expression of PP2Ac we also utilized an expression vector providing N-terminal HA-tag. The activity of the expressed PP2A was demonstrated by in vitro phosphatase assays and by specific inhibition of the enzyme by okadaic acid. Endothelial cells have low transfection efficiency [Tanner et al., 1997], which was confirmed by our observations too. On the other hand, according to the immunostaining pictures the recombinant protein was present in high concentration in the cells, which expressed the recombinant proteins. After all, we detected only about 30%–50% increase in PP2A activity compared to the appropriate controls. The cells containing either the recombinant PP2Ac or the recombinant PP2Aa and PP2Ac looked healthy and they did not differ from the neighboring (control) cells in term of shape, this suggests that the catalytic subunit was likely properly associated with native regulatory proteins; or with the recombinant A subunit. The recombinant A subunit can bind native B-subunit(s) and control the PP2A activity. The A subunit serves as a coordinator to assemble the catalytic C subunit and one of the B subunits of PP2A. The structure of the A subunit is quite well understood, the catalytic and the different B subunits bind to the A subunit at well-established

portions of the protein [Groves et al., 1999]. The regulatory B-subunit drives the PP2A holoenzyme to appropriate, native substrates, therefore we speculate that the recombinant C subunit binds to either native or recombinant regulatory A and endogenous B subunits. In agreement with this speculation, the recent publication of Strack et al. [2004] presents data
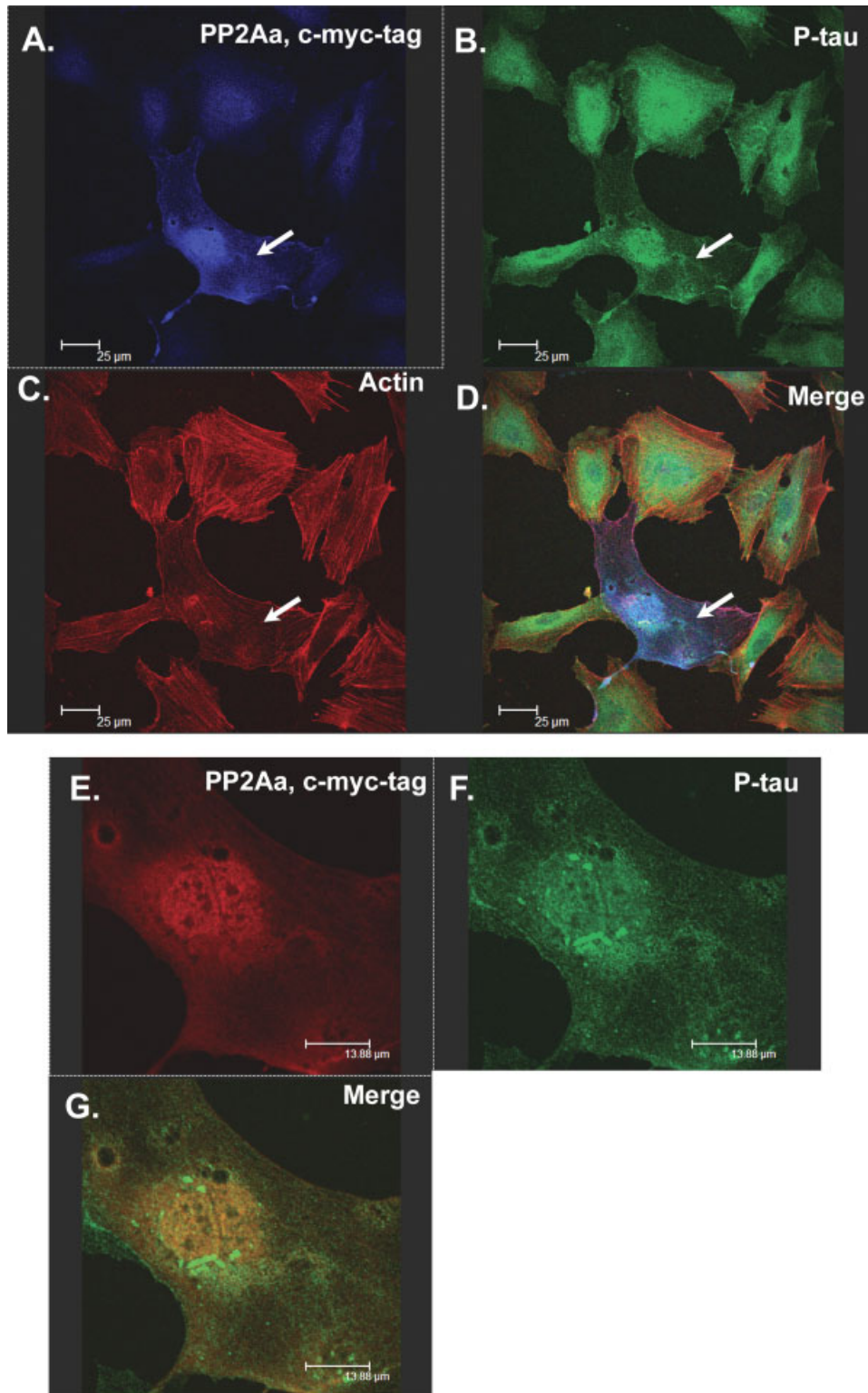

Fig. 12.

indicating the critical role of PP2A heterotrimers in mammalian cell survival.

The overexpression of PP2Ac and the co-expression of PP2Ac and PP2Aa rearranged the actin cytoskeleton as we demonstrated by immunofluorescent staining; it also led to a dramatic decrease in the amount of stress fibers in the cells and furthermore the peripheral actin region became thicker. Cortical actin assembly and thickening with enhanced TER was shown earlier in HPAEC and BPAEC upon sphingosine 1-phosphate, Sph-1-P, a lipid growth factor, treatment [Garcia et al., 2001]. Both PP2Ac and PP2Aa subunits seemed to co-localize with F-actin, this suggests protein–protein interactions between PP2A and actin or actin-binding protein(s). Association of PP2A with actin and other cytoskeletal proteins were also found in epithelial cells of the lung and of the kidney [Nunbhakdi-Craig et al., 2003]. The atrial G-protein-regulated inwardly rectifying K^+-channels are also assembled in a signaling complex containing PP2A and actin [Nikolov and Ivanova-Nikolova, 2004].

Although it is well-accepted that PP2A associates with MT/MAP [Sontag et al., 1995, 1999; Litersky et al., 1996; Gong et al., 2000, 2000a; Hiraga and Tamura, 2000; Kobayashi et al., 2001], the overexpression of PP2A did not significantly affect MT structure of quiescent EC. However, while nocodazole treatment destroyed MT structure in the non-overexpressing cell, PP2A overexpression preserved the MT network suggesting protective effect of PP2A activity on MT structure.

We and others have previously shown that both the MT-inhibitor nocodazole and the receptor-mediated edemagenic agonist, namely thrombin, induce a profound EC barrier dysfunction via rearrangement of F-actin cytoskeleton [Verin et al., 2001; Kawkitinarong et al., 2004]. Overexpression of active PP2A prevented or at least considerably reduced the effect of these agents on the F-actin. We can conclude that these data for the first time demonstrated the critical role of PP2A in maintaining EC cytoskeletal structure.

In order to directly examine the effect of PP2A on EC permeability, we generated recombinant adenoviral constructs of PP2Aa and PP2Ac subunits. We successfully infected EC with recombinant adenoviral constructs with approximately 100% transfection efficiency, as we demonstrated by Western blot analysis and immunofluorescent staining with specific antibodies. Infection of HPAEC with PP2Aa + c significantly attenuated the thrombin-, or the nocodazole-induced decrease in transendothelial electrical resistance. These novel data indicated that PP2A is directly involved in the EC barrier protection most likely via dephosphorylation of specific cytoskeletal targets, which results in the preservation of EC cytoskeleton.

To identify the physiological substrates for PP2A in EC cytoskeleton, first we focused on two cytoskeletal regulatory proteins, HSP27 and tau.

It was shown, that HSP27 has an effect on EC barrier regulation, via both actin stress fiber and focal adhesion formation [Schneider et al., 1998], and furthermore it has been also recognized as a potent regulator of cytoskeletal dynamics [Keezer et al., 2003]. Several studies have shown that overexpression of HSP27 increases the stability of F-actin microfilaments during the exposure to such stresses as hyperthermia, oxidants, and cytochalasin D [Lavoie et al., 1993; Huot et al., 1995; Guay et al., 1997], but the exact mechanism is poorly understood. However, the phosphorylation state of HSP27 determines its effect on actin polymerization [Benndorf et al., 1994; Gusev et al., 2002]. Non-phosphorylated small HSP monomers are active in inhibiting actin polymerization while phosphorylated monomers and non-phosphorylated oligomeric forms are inactive [Lavoie et al., 1993; Benndorf et al., 1994]. The majority of published data indicated that under non-stimulating conditions HSP27 is diffusely distributed

Fig. 12. PP2Ac overexpression attenuates tau phosphorylation evoked by thrombin treatment. HPAEC were co-transfected with PP2Ac/pCMV-HA and PP2Aa/pcDNA3.1 mammalian expression plasmids. The cells were treated with 20 nM thrombin for 30 min, and triple-stained to simultaneously visualize P-tau (green, **B** and **F**), F-actin (red, **C**), and PP2Aa (blue on **A**, BUT shown as red on **E**). Actin microfilaments were stained with Texas Red-phalloidin. Anti-phospho-tau (pS262) polyclonal and anti-c-myc-tag monoclonal antibodies were used to detect P-tau and PP2Aa, respectively. A–C are parallel images of the same set of triple-stained cells. Cell expressing PP2Ac and PP2Aa is shown by arrows; E, F are enlarged confocal images of this cell. D, G: merge of A–C or E, F, respectively, to show possible co-localization of phospho-tau, F-actin and PP2Aa, or phospho-tau and PP2Aa simultaneously. Shown are representative data of at least three independent experiments. [Color figure can be viewed in the online issue, which is available at www.interscience. wiley.com.]

in the cytoplasm [Miron et al., 1991; Loktionova et al., 1996, 1998; Loktionova and Kabakov, 1998; Wang and Bitar, 1998; Schafer et al., 1999], although according to other publications it is co-localized with actin [Ibitayo et al., 1999]. Recent in vivo results of Hirano et al. [2004] also suggest correlation between endothelial barrier dysfunction evoked by lipopolysaccharide with phosphorylation of HSP27.

HSP27 is a terminal substrate of the stress-activated p38 MAPK cascade [Armstrong et al., 1999; Gerthoffer and Gunst, 2001], but the dephosphorylation of HSPs is largely unexplored. A novel interaction between heat shock transcription factor 2 (HSF2) and the PR65/A subunit of PP2A was described and showed that HSF2 is able to compete with the PP2Ac for binding to PR65 [Hong and Sarge, 1999]. Others suggested that both PP2A and PP2B can dephosphorylate HSP27 in vitro. However, the in vivo phosphorylation level of HSP27 is affected when cells are treated with the inhibitors of PP1 and PP2A or with the inhibitor of PP2A, but with the inhibitor of PP2B. These findings suggest that PP2A is the key enzyme dephosphorylating HSP27 in the cells. The ability of PP2A to dephosphorylate HSP27 is shown to be regulated by the phosphorylation state of PP2A itself [Cairns et al., 1994].

Our immunoflourescent staining demonstrates that the treatment of EC with nocodazole or thrombin led to significant increase in HSP27 phoshorylation in nontransfected cells. On the other hand PP2A subunits overexpression significantly decreased the level of nocodazole/thrombin-induced HSP27 phosphorylation, which correlates with the protective effect of PP2A on EC barrier. Nocodazole-induced MT dissolution increased F-actin stress fiber formation only in the control, but it did not in the PP2A-transfected cells. This indicates the involvement of PP2A activity in the dynamic cross-talk between the actin cytoskeleton and the MT.

Microtubule-associated protein, tau, is an in vitro substrate for a number of protein kinases including p38 MAP kinase [Reynolds et al., 1997; Geschwind, 2003]. Tau has several isoforms, they are formed by alternative mRNA splicing of a single gene [Garcia and Cleveland, 2001]. Tau is predominantly found in neuronal cells, but it has been reported in several non-neuronal cells also including fibroblasts and lymphocytes [Cross et al., 1996; Ingelson et al.,

1996; Thurston et al., 1996]. Our data demonstrated that the transcript level of tau is the highest in HPAEC as compared to other investigated cell types. In its unphosphorylated form, tau promotes assembly of microtubules and inhibits the rate of depolymerization [Luduena et al., 1984; Drechsel et al., 1992]. Phosphorylation of tau by several kinases decreases its capacity to bind microtubules as well as to promote microtubule assembly [Singh et al., 1994; Litersky et al., 1996; Gupta and Abou-Donia, 1999]. Dephosphorylation of hyperphosphorylated tau restores its ability to promote microtubule assembly [Wang et al., 1995], thus, biological function of tau is regulated by phosphorylation. Our data indicate that the overexpression of PP2A significantly decreased the phosphorylation level of tau induced by nocodazole or thrombin. It correlates with the attenuation of nocodazole-induced cytoskeleton rearrangement and permeability. Moreover our data advocate co-localization of PP2A and tau in HPAEC. Collectively, these results suggest that both tau and HSP27 might be physiological cytoskeletal substrates of PP2A in endothelium, and they may be involved in PP2A-mediated EC barrier protection.

REFERENCES

Gong CX, Weigel J, Lidsky T, Zuck L, Avila J, Wisniewski HM, Grundke-Iqbal I, Iqbal K. 2000. Regulation of phosphorylation of neuronal microtubule-associated proteins MAP1b and MAP2 by protein phosphatase-2A and 2B in rat brain. Brain Res 853:299–309.

Armstrong SC, Delacey M, Ganote CE. 1999. Phosphorylation state of hsp27 and p38 MAPK during preconditioning and protein phosphatase inhibitor protection of rabbit cardiomyocytes. J Mol Cell Cardiol 31:555–567.

Baharians Z, Schonthal AH. 1998. Autoregulation of protein phosphatase type 2A expression. J Biol Chem 273:9019–19024.

Benndorf R, Hayess K, Ryazantsev S, Wieske M, Behlke J, Lutsch G. 1994. Phosphorylation and supramolecular organization of murine small heat shock protein HSP25 abolish its actin polymerization-inhibiting activity. J Biol Chem 269:20780–20784.

Birukov KG, Csortos C, Marzilli L, Dudek S, Ma SF, Bresnick AR, Verin AD, Cotter RJ, Garcia JG. 2001. Differential regulation of alternatively spliced endothelial cell myosin light chain kinase isoforms by p60(Src). J Biol Chem 276(11):8567–8573.

Birukova AA, Birukov KG, Smurova K, Adyshev D, Kaibuchi K, Alieva I, Garcia JG, Verin AD. 2004. Novel role of microtubules in thrombin-induced endothelial barrier dysfunction. FASEB J 18(15):1879–1890.

Cairns J, Qin S, Philp R, Tan YH, Guy GR. 1994. Dephosphorylation of the small heat shock protein Hsp27 in vivo by protein phosphatase 2A. J Biol Chem 269:9176–9183.

Clerk A, Michael A, Sugden PH. 1998. Stimulation of multiple mitogen-activated protein kinase sub-families by oxidative stress and phosphorylation of the small heat shock protein, HSP25/27, in neonatal ventricular myocytes. Biochem J 333:581–589.

Cohen P, Holmes CFB, Tsukitani Y. 1990. Okadaic acid: A new probe for the study of cellular regulation. Trends Biochem Sci 15:98–102.

Cross D, Tapia L, Garrido J, Maccioni RB. 1996. Tau-like proteins associated with centrosomes in cultured cells. Exp Cell Res 229:378–387.

Csortos C, Zolnierowicz S, Bako E, Durbin SD, DePaoli-Roach AA. 1996. High complexity in the expression of the B′ subunit of protein-phosphatase 2A₀. J Biol Chem 271:2578–2588.

Csortos C, Lazar V, Garcia JGN. 1999. Screening cDNA libraries using partial probes to isolate full-length cDNAs from vascular cells. In: Baker AH, editor. Methods in Mol Med, Vol. 30: Vascular disease: Mol Biol and gene therapy protocols Humana Press, Inc. Totowa, pp 59–72.

Dejana E. 2004. Endothelial cell-cell junctions: Happy together. Nature Rev 5:261–271.

Diwan AH, Honkanen RE, Schaeffer RC, Jr., Strada SJ, Thompson WJ. 1997. Inhibition of serine-threonine protein phosphatases decreases barrier function of rat pulmonary microvascular endothelial cells. J Cell Physiol 171:259–270.

Drechsel DN, Hyman AA, Cobb MH, Kirschner MW. 1992. Modulation of the dynamic instability of tubulin assembly by the microtubule-associated protein tau. Mol Biol Cell 3(10):1141–1154.

Dudek SM, Garcia JGN. 2001. Cytoskeletal regulation of pulmonary vascular permeability. J Appl Physiol 91:1487–1500.

Erdodi F, Toth B, Hirano K, Hirano M, Hartshorne DJ, Gergely P. 1995. Endothall thioanhydride inhibits protein phosphatases-1 and -2A in vivo. Am J Physiol 269:C1176–C1184.

Ferhat L, Represa A, Bernard A, Ben-ari Y, Khrestchatisky M. 1996. MAP2d promotes bundling and stabilization of both microtubules and microfilaments. J Cell Sci 109:1095–1103.

Gabel S, Benefield J, Meisinger J, Petruzzelli GJ, Young M. 1999. Protein phosphatasaes 1 and 2A maintain endothelial cells in a resting state, limiting the motility that is needed for the morphogenic process of angiogenesis. Otolaryngol Head Neck Surg 121:463–468.

Garcia ML, Cleveland DW. 2001. Going new places using an old MAP: Tau, microtubules and human neurodegenerative disease. Curr Opin Cell Biol 13:41–48.

Garcia JGN, Birnboim AS, Del Vecchio PJ, Fenton JW, Malik AB. 1986. Thrombin-induced increases in albumin clearance across cultured endothelial monolayers. J Cell Physiol 128:96–104.

Garcia JGN, Davis HW, Patterson CE. 1995. Regulation of endothelial cell gap formation and barier dysfunction: Role of myosin light chain phophorylation. J Cell Physiol 163:510–522.

Garcia JGN, Schaphorst KL, Shi S, Verin AD, Hart CM, Callahan KS, Patterson CE. 1997. Mechanisms of ionomycin-induced endothelial cell barrier dysfunction. Am J Physiol Lung Cell Mol Physiol 273:L172–L184.

Garcia JGN, Liu F, Verin AD, Birukova A, Dechert MA, Gerthoffer WT, Bamburg JR, English D. 2001. Sphingosine 1-phosphate promotes endothelial cell barrier integrity by Edg-dependent cytoskeletal rearrangement. J Clin Invest 108(5):689–701.

Gerthoffer WT, Gunst SJ. 2001. Invited review: Focal adhesion and small heat shock proteins in the regulation of actin remodeling and contractility in smooth muscle. J Appl Physiol 91:963–972.

Geschwind DH. 2003. Tau phosphorylation, tangles, and neurodegeneration: The chicken or the egg? Neuron 40:457–460.

Giaever I, Keese CR. 1993. A morphological biosensor for mammalian cells. Nature 366:591–592.

Gong CX, Lidsky T, Wegiel J, Zuck L, Grundke-Iqbal I, Iqbal K. 2000a. Phosphorylation of microtubule-associated protein tau is regulated by protein phosphatase 2A in mammalian brain. J Biol Chem 275:5535–5544.

Graham FL, Smiley J, Russell WC, Nairn R. 1977. Characteristics of a human cell line transformed by DNA from human adenovirus type 5. J Gen Virol 36(1):59–74.

Groves MR, Hanlon N, Turowski P, Hemmings BA, Barford D. 1999. The structure of the protein phosphatase 2A PR65/A subunit reveals the conformation of its 15 tandemly repeated HEAT motifs. Cell 96:99–110.

Guay J, Lambert H, Gingras-Breton G, Lavoie JN, Huot J, Landry J. 1997. Regulation of actin filament dynamics by p38 map kinase-mediated phosphorylation of heat shock protein 27. J Cell Sci 110:357–368.

Gupta RP, Abou-Donia MB. 1999. Tau phosphorylation by diisopropil phosphorofluoridate (DFP)-treated hen brain supernatant inhibits its binding with microtubules: Role of Ca²⁺/calmodulin-dependent protein kinase II in tau phosphorylation. Arch Biochem Biophys 365:268–278.

Gusev NB, Bogatcheva NV, Marston SB. 2002. Structure and properties of small heat shock proteins (sHsp) and their interaction with cytoskeleton proteins. Biochemistry (Mosc) 67:511–519.

Hartshorne DJ, Ito M, Erdodi F. 1998. Myosin light chain phosphatase: Subunit composition, interactions and regulation. J Muscle Res Cell Motil 19(4):325–341.

He TC, Zhou S, da Costa LT, Yu J, Kinzler KW, Vogelstein B. 1998. A simplified system for generating recombinant adenoviruses. Proc Natl Acad Sci USA 95:2509–2514.

Hedges JC, Dechert MA, Yamboliev IA, Martin JL, Hickey E, Weber LA, Gerthoffer WT. 1999. A role for p38

(MAPK)/HSP27 pathway in smooth muscle cell migration. J Biol Chem 274:24211–24219.

Hiraga A, Tamura S. 2000. Protein phosphatase 2A is associated in an inactive state with microtubules through 2A1-specific interaction with tubulin. Biochem J 346: 433–439.

Hirano S, Rees RS, Yancy SL, Welsh MJ, Remick DG, Yamada T, Hata J, Gilmont RR. 2004. Endothelial barrier dysfunction caused by LPS correlates with phosphorylation of HSP27 in vivo. Cell Biol Toxicol 20: 1–14.

Hong Y, Sarge KD. 1999. Regulation of protein phosphatase 2A activity by heat shock transcription factor 2. J Biol Chem 274:12967–12970.

Huot J, Lambert H, Lavoie JN, Guimond A, Houle F, Landry J. 1995. Characterization of 45-kDa/54-kDa HSP27 kinase, a stress-sensitive kinase which may activate the phosphorylation-dependent protective function of mammalian 27-kDa heat-shock protein HSP27. Eur J Biochem 227:416–427.

Huot J, Houle F, Marceau F, Landry J. 1997. Oxidative stress-induced actin reorganization mediated by the p38 mitogen-activated protein kinase/heat shock protein 27 pathway in vascular endothelial cells. Circ Res 80(3): 383–392.

Ibitayo AL, Sladick J, Tuteja S, Louis-Jacques O, Yamada H, Groblewski G, Welsh M, Bitar KN. 1999. HSP27 in signal transduction and association with contractile proteins in smooth muscle cells. Am J Physiol 277: G445–G454.

Ingelson M, Vanmechelen E, Lannfelt L. 1996. Microtubule-associated protein tau in human fibroblasts with the Swedish Alzheimer mutation. Neurosci Lett 220: 9–12.

Ishikawa R, Kagami O, Hayasi C, Kohama K. 1992. Characterization of smooth muscle caldesmon as a microtubule-associated-protein. Cell Motil Cytoskeleton 23:244–251.

Janssens V, Goris J. 2001 . Protein phosphatase 2A: A highly regulated family of serine/threonine phosphatases implicated in cell growth and signalling. Biochem J 353(Pt 3):417–439.

Kawkitinarong K, Linz-McGillem L, Birukov KG, Garcia JGN. 2004. Differential regulation of human lung epithelial and endothelial barrier function by thrombin. Am J Respir Cell Mol Biol 31(5):517–527.

Keezer SM, Ivie SE, Krutzsch HC, Tandle A, Libutti SK, Roberts DD. 2003. Angiogenesis inhibitors target the endothelial cell cytoskeleton through altered regulation of heat shock protein 27 and cofilin. Cancer Res 63:6405–6412.

Kiss E, Muranyi A, Csortos C, Gergely P, Ito M, Hartshorne DJ, Erdodi F. 2002. Integrin-linked kinase phosphorylates the myosin phosphatase target subunit at the inhibitory site in platelet cytoskeleton. Biochem J 365 (Pt 1):79–87.

Knapp J, Boknik P, Luss I, Huke S, Linck B, Luss H, Muller FU, Muller T, Nacke P, Noll T, Piper HM, Schmitz W, Vahlensieck U, Neumann J. 1999. The protein phosphatase inhibitor cantharidin alters vascular endothelial cell permeability. J Pharmacol Exp Ther 289:1480–1486.

Kobayashi N, Reiser J, Schwarz K, Sakai T, Kriz W, Mundel P. 2001. Process formation of podocytes: Morphogenetic activity of microtubules and regulation by

protein serine/threonine phosphatase PP2A. Histochem Cell Biol 115:255–266.

Kolosova IA, Csortos C, Garcia JGN, Verin AD. 2003. Role of Ser/Thr protein phosphatases in endothelial cytoskeletal organization and barrier function. Recent Res Devel Physiol 1:385–400.

Kolosova IA, Ma SF, Adyshev DM, Wang P, Ohba M, Natarajan V, Garcia JG, Verin AD. 2004. Role of CPI-17 in the regulation of endothelial cytoskeleton. Am J Physiol Lung Cell Mol Physiol 287(5):L970–L980.

Laemmli UK. 1970. Cleavage of structural proteins during the assembly of the head of bacteriophage T4. Nature 227:680–685.

Larsen JK, Yamboliev IA, Weber LA, Gerthoffer WT. 1997. Phosphorylation of the 27-kDa heat shock protein via p38 MAP kinase and MAPKAP kinase in smooth muscle. Am J Physiol 273:L930–L940.

Lavoie JN, Gingras-Breton G, Tanguay RM, Landry J. 1993. Induction of Chinese hamster HSP27 gene expression in mouse cells confers resistance to heat shock. HSP27 stabilization of the microfilament organization. J Biol Chem 268:3420–3429.

Lavoie JN, Lambert H, Hickey E, Weber LA, Landry J. 1995. Modulation of cellular thermoresistance and actin filament stability accompanies phosphorylation-induced changes in the oligomeric structure of heat shock protein 27. Mol Cell Biol 15:505–516.

Lee TY, Gotlieb AI. 2003. Microfilaments and microtubules maintain endothelial integrity. Microsc Res Tech 60: 115–127.

Litersky JM, Johnson GVW, Jakes R, Goedert M, Lee M, Seubert P. 1996. Tau protein is phophorylated by cyclic AMP-dependent protein kinase and calcium/calmodulin-dependent protein kinase II within its microtubule-binding domains at Ser-262 and Ser-356. Biochem J 316:655–660.

Loktionova SA, Kabakov AE. 1998. Protein phosphatase inhibitors and heat preconditioning prevent Hsp27 dephosphorylation, F-actin disruption and deterioration of morphology in ATP-depleted endothelial cells. FEBS Lett 433:294–300.

Loktionova SA, Ilyinskaya OP, Gabai VL, Kabakov AE. 1996. Distinct effects of heat shock and ATP depletion on distribution and isoform patterns of human Hsp27 in endothelial cells. FEBS Lett 392:100–104.

Loktionova SA, Ilyinskaya OP, Kabakov AE. 1998 . Early and delayed tolerance to simulated ischemia in heat-preconditioned endothelial cells: A role for HSP27. Am J Physiol 275:H2147–H2158.

Lontay B, Serfozo Z, Gergely P, Ito M, Hartshorne DJ, Erdodi F. 2004. Localization of myosin phosphatase target subunit 1 in rat brain and in primary cultures of neuronal cells. J Comp Neurol 478(1):72–87.

Luduena RF, Fellous A, McManus L, Jordan MA, Nunez J. 1984. Contrasting roles of tau and microtubule-associated protein 2 in the vinblastine-induced aggregation of brain tubulin. J Biol Chem 259:12890–12898.

Miron T, Vancompernolle K, Vandekerckhove J, Wilchek M, Geiger B. 1991. A 25-kD inhibitor of actin polymerization is a low molecular mass heat shock protein. J Cell Biol 114:255–261.

Moraga DM, Nunez P, Garrido J, Maccioni RB. 1993. A tau fragment containing a repetitive sequence induces bundlig od actin filaments. J Neorochem 61:979–986.

Nikolov EN, Ivanova-Nikolova TT. 2004. Coordination of membrane excitability through a GIRK1 signaling complex in the atria. J Biol Chem 279:23630–23636.

Nunbhakdi-Craig V, Craig L, Machleidt T, Sontag E. 2003. Simian virus 40 small tumor antigen induces deregulation of the actin cytoskeleton and tight junctions in kidney epithelial cells. J Virol 77:2807–2818.

Petrache I, Birukova A, Ramirez SI, Garcia JGN, Verin AD. 2003. The role of the microtubules in tumor necrosis factor-alpha-induced endothelial cell permeability. Am J Respir Cell Mol Biol 28:574–581.

Reynolds CH, Nebreda AR, Gibb GM, Utton MA, Anderton BH. 1997. Reactivating kinase/p38 phosphorylates tau protein in vitro. J Neurochem 69:191–198.

Satillaro RF, Dentler WL, Le Cluyse EL. 1981. Microtubule-associated proteins (MAPs) and the organization of actin filaments in vitro. J Cell Biol 90:467–473.

Schafer C, Ross SE, Bragado MJ, Groblewski GE, Ernst SA, Williams JA. 1998. A role for the p38 mitogen-activated protein kinase/Hsp 27 pathway in cholecystokinin-induced changes in the actin cytoskeleton in rat pancreatic acini. J Biol Chem 273:24173–24180.

Schafer C, Clapp P, Welsh MJ, Benndorf R, Williams JA. 1999. HSP27 expression regulates CCK-induced changes of the actin cytoskeleton in CHO-CCK-A cells. Am J Physiol 277:C1032–C10343.

Schaphorst KL, Pavalko FM, Patterson CE, Garcia JGN. 1997. Thrombin-mediated focal adhesion plaque reorganization in endothelium: Role of protein phosphorylation. Am J Respir Cell Mol Biol 17:443–455.

Schneider GB, Hamano H, Cooper LF. 1998. In vivo evaluation of hsp27 as an inhibitor of actin polymerization: hsp27 limits actin stress fiber and focal adhesion formation after heat shock. J Cell Physiol 177:575–584.

Singh TJ, Grundke-Iqbal I, McDonald B, Iqbal K. 1994. Comparison of the phosphorylation of microtubule-associated protein tau by non-proline dependent protein kinases. Mol Cell Biochem 131:181–189.

Sontag E, Nunbhakdi-Craig V, Bloom GS, Mumby MC. 1995. A novel pool of protein phosphatase 2A is associated with microtubules and is regulated during the cell cycle. J Cell Biol 128:1131–1144.

Sontag E, Nunbhakdi-Craig V, Lee G, Brandt R, Kamibayashi C, Kuret J, White CL, Mumby MC, Bloom GS. 1999. Molecular interactions among protein phosphatase 2A, tau, and microtubules. Implications for the regulation of tau phophorylation and development of taupathies. J Biol Chem 274:25490–25498.

Strack S, Cribbs JT, Gomez L. 2004. Critical role for protein phosphatase 2A heterotrimers in mammalian cell survival. J Biol Chem 279(46):47732–47739.

Tanner FC, Carr DP, Nabel GJ, Nabel EG. 1997. Transfection of human endothelial cells. Cardiovasc Res 35:522–528.

Tar K, Birukova AA, Csortos C, Bako E, Garcia JGN, Verin AD. 2004. Phosphatase 2A is involved in endothelial cell microtubule remodeling and barrier regulation. J Cell Biochem 92(3):534–546.

Thurston VC, Zinkowski RP, Binder LI. 1996. Tau as a nucleolar protein in human nonneural cells in vitro and in vivo. Chromosoma 105:20–30.

Togel M, Wiche G, Propst F. 1998. Novel features of the light chain of microtubule-associated protein MAP1B: Microtubule stabilization, self interaction, actin filament binding, and regulation by the heavy chain. J Cell Biol 143:695–707.

Towbin H. Staehelin T, Gordon J. 1992. Electrophoretic transfer of proteins from polyacrylamide gels to nitrocellulose sheets: Procedure and some applications. Biotechnology 24:145–149.

Verin AD, Patterson CE, Day MA, Garcia JGN. 1995. Regulation of endothelial cell gap formation and barrier function by myosin-associated phosphatase activities. Am J Physiol 269:L99–L108.

Verin AD, Lazar V, Torry RJ, Labarrere CA, Patterson CE, Garcia JGN. 1998. Expression of a novel high molecular weight myosin light chain kinase in endothelium. Am J Respir Cell Mol 19:758–766.

Verin AD, Csortos C, Durbin SD, Aydanyan A, Wang P, Patterson CE, Garcia JG. 2000. Characterization of the protein phosphatase 1 catalytic subunit in endothelium: Involvement in contractile responses. J Cell Biochem 79:113–125.

Verin AD, Birukova A, Wang P, Liu F, Becker P, Birukov KG, Garcia JGN. 2001. Microtubule disassembly increases endothelial cell barrier dysfunction: Role of MLC phosphorylation. Am J Physiol Lung Cell Mol Physiol 281(3):L565–L574.

Wadzinski BE, Eisfelder BJ, Peruski LF, Jr., Mumby MC, Johnson GL. 1992. NH$_2$-terminal modification of the phosphatase 2A catalytic subunit allows functional expression in mammalian cells. J Biol Chem 267:16883–16888.

Wang P, Bitar KN. 1998. Rho A regulates sustained smooth muscle contraction through cytoskeletal reorganization of HSP27. Am J Physiol 275:G1454–G1462.

Wang JZ, Gong CX, Zaidi T, Grundke-Iqbal I, Iqbal K. 1995. Dephosphorylation of Alzheimer paired helical filaments by protein phosphatase-2A and -2B. J Biol Chem 270:4854–4860.

Wera S, Hemmings BA. 1995. Serine-threonine protein phosphatases. Biochem J 311:17–29.

Yansong Li, Jiali Liu, Xi Zhan. 2000. Tyrosine Phosphorylation of Cortactin Is Required for H$_2$O$_2$-mediated Injury of Human Endothelial Cells. J Biol Chem 275(47):37187–37193.